Numerical Model of Eddy Current Inspection with DC Magnetic Field Associated

J.V. Rocha[1], C. Camerini[1,*], R.W.F. Santos[2], V.M. Silva[1], Lucas B. Campos[1] and G.R. Pereira[1]

[1]*Laboratory of Non-Destructive Testing, Corrosion and Welding, Department of Metallurgical and Materials Engineering, Federal University of Rio de Janeiro, Brazil*

[2]*Petrobras Research and Development Center, Rio de Janeiro, Brazil*

Abstract: Most non-destructive techniques can be well represented in a virtual environment, in particular, eddy current testing (ECT) simulation is a useful and well-established tool to predict and represent real inspection situations permitting testing customization in a fast, cheap and efficient way. Conventional ECT generally works with low-intensity magnetic fields, however, for advanced variations of the technique, where external DC magnetic fields can be applied to locally decrease the magnetic permeability, there is no Finite Element Method (FEM) packages available to deal with such nonstandard model. Many authors [1] and [2] have presented this ECT solution for different industrial applications using external DC magnetization to carry nonlinear ferromagnetic materials to the saturation level of the magnetization curve to increase the ECT depth penetration. In general, ECT modelling calculation is benefited by properties of steady-state regime where all magnetic fields are oscillating at the same frequency not permitting through multi-frequency calculation. The present work proposes a simulation solution for such a case where DC magnetic field is associated with ECT. A theoretical model is presented together with experimental results validation.

Keywords: Eddy current testing, External DC magnetic field, Material inspection.

1. INTRODUCTION

Eddy current testing (ECT) is a widely used non-destructive technique to evaluate materials in many industries scenarios. Aircraft, nuclear and petrochemical industries are examples where ECT plays a key role in ensuring components integrity. The method is based on the detection of coil impedance change due to eddy currents induced on the test specimen [3-7]. The presence of a defect modifies the eddy current pattern which gives rise to a field perturbation and hence changes the coil impedance.

From the industry point of view, it is relevant to have a dedicated simulation tool to reliably represent real inspection situations in a virtual environment. In this way, several works have addressed methodologies of computational analysis aiming at the validation of experiments and customization of ECT sensors [8-11], resulting though in a few FEM commercial software for the standard ECT application. However, conventional ECT generally works with low-intensity magnetic fields and for advanced variations of the technique, where external DC magnetic fields can be applied to locally decrease the magnetic permeability, there are no FEM packages available to deal with such a nonstandard model. In general, ECT modelling calculation is benefited by properties of steady-state regime where all magnetic fields are oscillating at the same frequency not permitting through multi-frequency calculation. Many scientific efforts have been deposited to overcome the limitations of the existing ECT FEM packages. Cuihua Tian *et al*. computationally evaluated demagnetization in NdFeB permanent magnets present in saturated core fault current limiter (SCFCL) proved by eddy currents [12]. For this, a finite element analysis was performed in order to obtain the transient configuration of the SCFCL, then the expression of the flow density was obtained by adjusting the curve and, finally, the losses were calculated using the analytical model. Works related to the inspection area by non-destructive techniques presented by Fabrice Foucher *et al.* [13], Zhiyang Deng *et al*. [14] and Satoru Horai *et al*. [15] show the use of finite element analysis methods for the case of eddy currents with magnetic saturation through an external DC field. These were developed by separating the problem into two stages, in the first it analyzed only the interaction of the DC field with the material in order to obtain the distribution of magnetic permeability. Then eddy current inspection simulations were performed for the permeability settings obtained in the first stage. However, due to the focus of the works being the results of the inspection of the simulation, it is not presented in details of the mathematical formulation of the methodology.

*Address correspondence to this author at the Laboratory of Non-Destructive Testing, Corrosion and Welding, Department of Metallurgical and Materials Engineering, Federal University of Rio de Janeiro, Brazil;
E-mail: change.cgcamerini@metalmat.ufrj.br

E-ISSN: 2410-4701/21

The present work proposes a simulation solution for such a case where DC magnetic field is associated with conventional ECT. A theoretical model is presented together with experimental results validation. ECT in combination with DC magnetic field improves ferromagnetic materials inspection. Eddy currents have a small penetration depth in ferromagnetic materials due to high relative magnetic permeability, this limited penetration is known as the "skin effect" [16, 17] and it can be reduced by imposing a DC magnetization which locally reduces the magnetic relative permeability of the material and increases the eddy current depth penetration, permitting inspection of thicker components [18]. Besides the enlargement of depth penetration, the imposed DC magnetic field lines in case of a defect have a higher concentration density in the remaining wall thickness which consequently changes the relative permeability in the area and changes the eddy current field lines. Figure **1** presents the experimental set-up schematic consisted of a magnetic circuit employing two permanent magnets, the test piece, a U-shaped piece of low carbon steel to close the magnetic circuit and the ECT probe between the magnets. In case of a defect the magnetic field lines are concentrated in the remaining wall, increasing the magnetic flux and changing the eddy current field lines.

2. EQUATIONS

To simulate ECT with DC magnetic field associated is important to understand the governing equations of each situation separately. The DC magnetic field is calculated by using magnetostatic equations present in section 2.1 whereas ECT modelling is benefited by properties of the steady-state regime shown in section 2.2.

2.1. Magneto-Static

The FEM simulation magnetostatic model can be divided into three regions for a better understanding. The first one is the region of interest, which includes the NdFeB magnets, the inspection sample, and a U-shape metal to close the magnetic circuit, all have nonzero conductivity, permittivity, or permeability. The second space is the air surrounding the whole model, which is considered as free space. The last one is the outer boundaries. As with all electromagnetic modelling, the basis comes from Maxwell's Equations [17].

From Ampere:

$$\nabla \mathbf{x}\mathbf{H} = \mathbf{J} + \frac{\partial \mathbf{D}}{\partial t} \tag{1}$$

From Faraday:

$$\nabla \mathbf{x}\mathbf{E} = -\frac{\partial \mathbf{B}}{\partial t} \tag{2}$$

From Gauss:

$$\nabla . \mathbf{D} = \rho \tag{3}$$

$$\nabla . \mathbf{B} = 0 \tag{4}$$

The fields $\mathbf{B}$ and H have a non-linear relationship with each other so that the equality is founded through μ which is also dependent on the field (Eq. 5):

$$\mathbf{B} = \mu \mathbf{H} \tag{5}$$

The magnetic scalar potential is defined according to equation 6, where the ψ represents the (total) scalar potential.

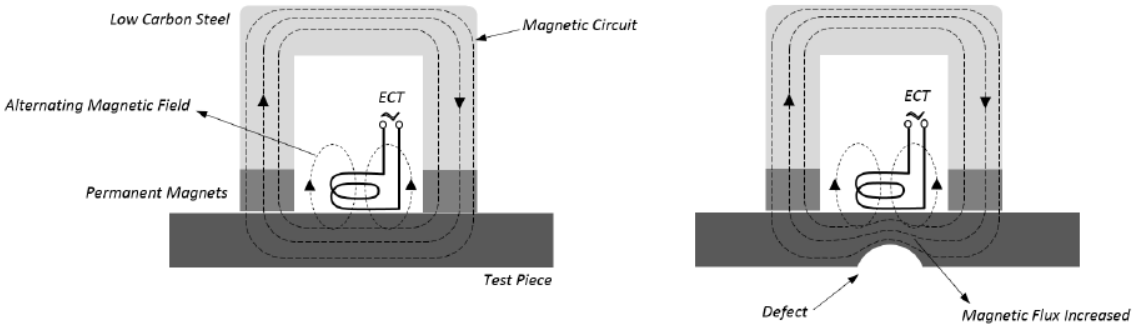

Figure 1: Experimental set-up schematic of ECT with DC magnetic field associated.

$$\mathbf{H} = -\nabla\psi \tag{6}$$

In one dimension:

$$\mathbf{H} = -\frac{\partial\psi}{\partial x} \tag{7}$$

Combining Eq. (6), Eq. (5) and Eq. (4):

$$-\nabla.\mu\nabla\psi = 0 \tag{8}$$

This is the equation used for modelling Magnetostatics problems in the absence of electric currents. Finding ψ allows $\mathbf{B}$ and $\mathbf{H}$ to be determined.

2.2. Steady State

Starting with Maxwell's equations as in equations 1-4. In a linear and isotropic environment in which the physical properties, such as, magnetic permeability μ, electric conductivity σ and permittivity ϵ do not depend on the direction, it is possible to assume some relations like Eq. (5), $\mathbf{D} = \epsilon\mathbf{E}$ and the current density can be written as $\mathbf{J} = \sigma\mathbf{E}$.

After manipulating the Maxwell equations in its differential derivative form, one can reach the differential diffusion that governs the pattern of eddy currents in conducting materials (Eq. 09) [19].

$$\nabla\frac{1}{\mu}x(\nabla x\mathbf{A}) = \mathbf{J}_s - \sigma\frac{\partial\mathbf{A}}{\partial t} \tag{9}$$

Where:

μ: magnetic permeability [H/m].

A: magnetic potencial vector [Weber/m].

$\mathbf{J}_s$: inducted current vector [A/m^2].

σ: electrical conductivity [S/m].

For the linear case, when the coil is excited by a sinusoidal wave, the equation 09 can be reduced to:

$$\nabla\frac{1}{\mu}x(\nabla x\mathbf{A}) = \mathbf{J}_s + j\omega\sigma\mathbf{A} \tag{10}$$

Where:

ω: angular frequency [rad/s].

The solution of this linear diffusion equation when the excitation is sinusoidal can be achieved in terms of A, solving the Eq. 10 taking care of the contour conditions. With the values of A calculated, it is possible to obtain many electromagnetic features, such as: energy dissipation, magnetic flux density and impedance variation of the eddy current coil [19].

3. MODEL DEFINITION

It is not possible to deal with magneto-static and ECT Steady State equations at the same simulation model. As noticed by the equations, the magneto-static model does not consider oscillating magnetic fields while ECT Steady State does not support multi-frequency calculation. To solve this conflict two solutions were considered, the time Domain Solution and Superposition solution.

3.1. Time Domain Solution

The first approach to solve this problem is to use a time-domain solution instead of a time-harmonic solution. That way it is possible to consider as many frequencies as necessary in the same solution, but on the other hand, many calculations must be made incrementing time with a small-time step with at least twenty points per cycle in order to have a sufficient sample rate. This approach is widely used in Pulsed Eddy Current (PEC) simulation, as the rectangular pulse is a combination of several frequencies [20]. Combine that and the high frequencies that are usually used in ECT and the simulation process becomes computationally slow and expensive. It is worth mentioning that the main objective of this paper is to work around this limitation and propose a new solution using superposition of just two simulations, firstly a magneto-static and then an ECT steady state.

3.2. Superposition Solution

In this alternative solution the main goal is to achieve the same results as the transient solution, but with a less computational resource. In order to do it, some assumptions must be made. First, both the solutions must have a linear relationship between other, second, the oscillating field excited by the coil must be sufficiently small that it can be considered as a perturbation that does not affect the magnetic saturation of the sample. This solution idea comes directly from the electric circuit and linear system theories where it is possible to compute multiple sources contributions by calculating each one individually and just after all computations combine

them, such approach was also applied in previous ECT papers [21]. Consequently, it is possible to import the permeability distribution from the static model to the dynamic steady-state model.

4. MODEL DEFINITION

Opera 3D from Vector Fields Cobham was the simulation software and the model to be solved is a horseshoe type magnet with permanent magnet NdFeB poles and SAE 1020 steel. The plate, testing sample, of duplex stainless steel completes the magnetic circuit, as shown in Figure **2**.

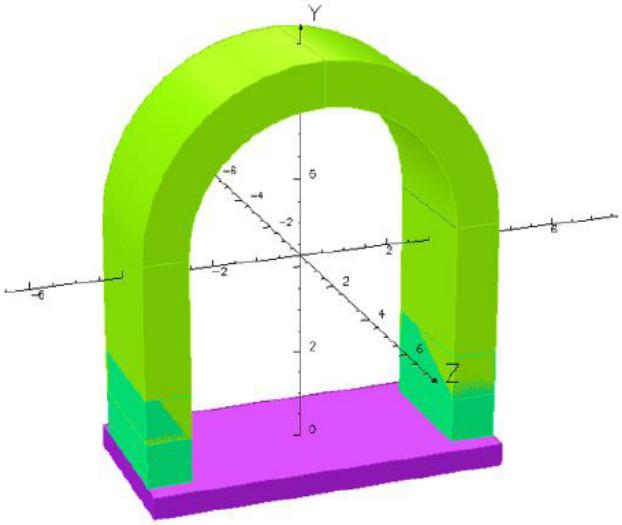

Figure 2: Horseshoe magnet setup for statics solving.

Because of the symmetry of the model, it is possible to solve just one-quarter of the structure. The tangential magnetic boundary condition is applied to the XY plane and the normal magnetic boundary condition to the YZ plane. Magnetic saturation causes the permeability in the duplex steel to be non-uniform, as shown in Figure **3**. The contours are obtained by plotting component B/H (CGS units).

The quality of the duplex steel is accessed via ECT, by applying an AC field to the sample using a coil. As pointed before, this perturbation does not affect the magnetic saturation of the duplex sample. Consequently, it is possible to use the information of the magnetic permeability in the saturation state given by the magnetostatic solution.

The duplex sample plate in the steady-state solution must have the same geometry like the one in the statics solution. After the mesh is done in this sample it is possible to create a table that contains x, y and z coordinates for all the element centroids for the whole mesh. These coordinates will serve as inputs values for the permeability table that is going to be used for the steady-state solution. It is possible to see the magnetic permeability values imported to the Steady State model in Figure **4**, note that because there is just one permeability value for each mesh element the image is more pixeled than in Figure **3**.

After all the calculations are done, it is possible to see the induced current pattern as in Figure **5**. The

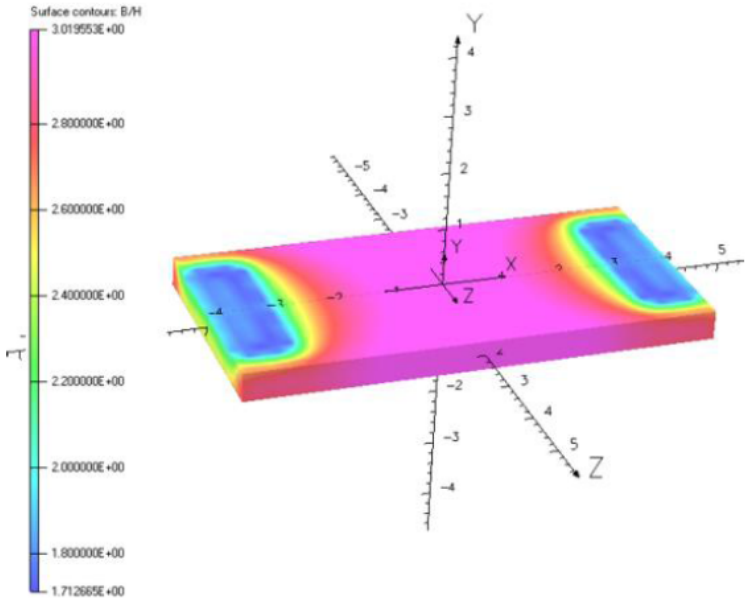

Figure 3: Horseshoe magnet solved in non-linear Statics.

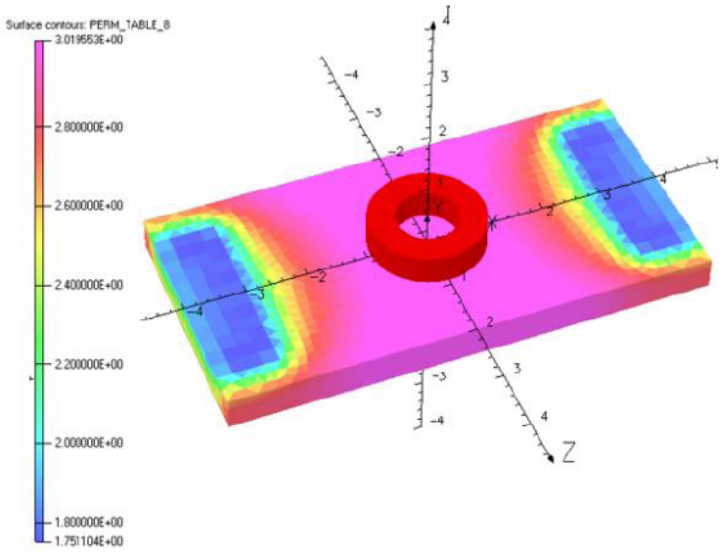

Figure 4: Imported magnetic permeability distribution.

results are obtained by analyzing the impedance of the coil that changes when it approaches the conductive media that is being tested. To represent the coil approach to the testing piece three simulations with liftoff (distance of the sensor from the testing sample) of 0.5, 2 and 5 millimetres have been made, as can be seen in Figure **6**.

Once the impedance is a complex number, the resistance, real part, is computed with the Joule Losses (Equation 11) and the inductive reactance, imaginary part, is computed with the magnetic energy (Equation 12) both calculations are done within the whole meshed domain, as in [22].

$$Re(\Delta Z) = \frac{\int_{\Omega_c} \frac{1}{\sigma}(|\mathbf{J}_f^2| - |\mathbf{J}^2|)d\Omega_c}{I^2} \quad (11)$$

$$Im(\Delta Z) = \frac{\int_{\Omega_c} \frac{1}{\mu}(|\mathbf{B}_f^2| - |\mathbf{B}^2|)d\Omega_c}{\omega * I^2} \quad (12)$$

Where:

Jf and J are the current density field with and without the defect, respectively.

Bf and B are the magnetic induction field with and without the defect, respectively.

I is the applied electric current.

ω is the angular frequency.

Previous experimental results [2] showed that this variation of the ECT technique (with external DC

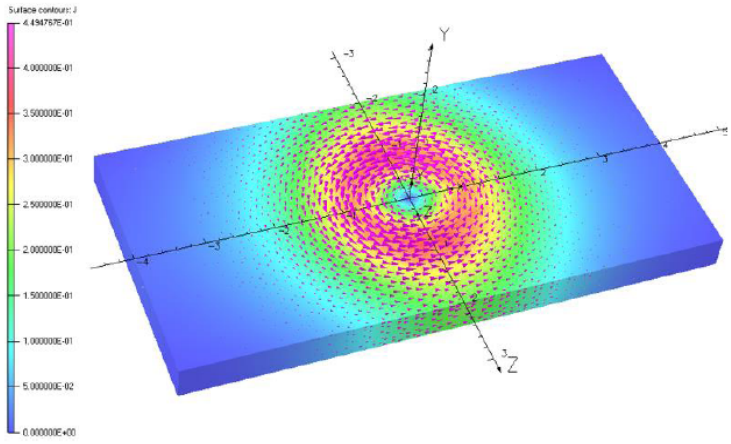

Figure 5: Eddy current pattern after solving.

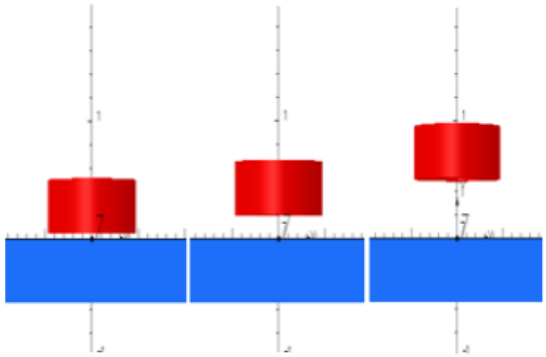

Figure 6: Three different liftoff of 0.5, 2 and 5 millimeters to simulate the probe approaching the specimen.

magnetization) was capable of sorting through different types of duplex stainless steel whereas the conventional ECT could not. Unfortunately, it is not possible to validate the results in a numerical manner. This happens because the eddy current equipment used to make the measures uses digital tools to enhance the signal, such as: digital filters, overall gain and vertical gain. The way these tools are utilized is not explicit in the equipment datasheet. In this way, the comparison between the results obtained by the simulation and by the experimental measures was made qualitatively through the morphology of the signals and in the ability to distinguish the different specimens. In this way it was just possible to validate the results by comparing them qualitatively. The agreement between the simulated and experimental results is good enough as can be seen in Figures **7** and **8**. The simulated results as well as the experimental results could sort the different types of duplex stainless steel successfully.

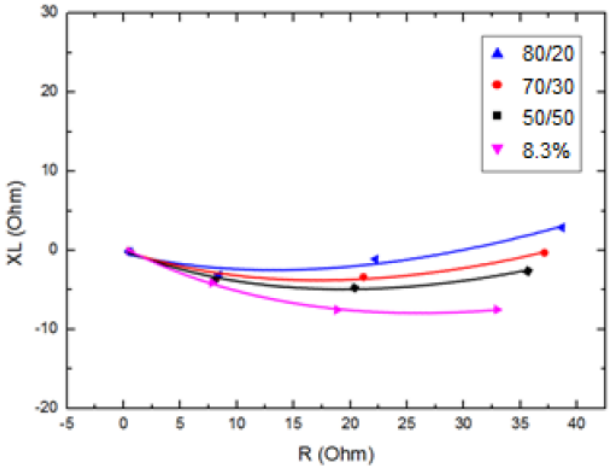

Figure 7: Simulation results.

The reference samples have been solubilized at 1120° C for 1 hour and water quenched in order to contain approximately 50% of ferrite and 50% of austenite and is indicated in the graphic legend as 50/50. Further heat treatments were conducted to obtain unbalanced microstructures with 80% and 70% of ferrite and 20% and 30% of austenite, and 8.3% of sigma phase. The heat treatments parameters to obtain each of the tested microstructure are detailed by Camerini *et al*. [2].

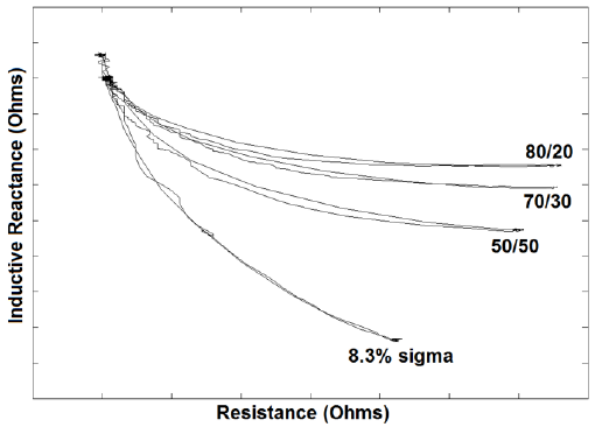

Figure 8: Experimental results of duplex stainless-steel sorting using ECT with external DC magnetic field.

5. CONCLUSION

Based on the advantages of use ECT associated with DC magnetization, a novel numerical model solution was presented to simulate and predict the interaction between the alternate and constant magnetic field. The results showed the magnetic permeability variation caused by the imposed DC magnetic field and using the superposition solution ECT inspection could be evaluated in the presence of external DC magnetic fields.

The simulation results presented the possibility to evaluate metallurgical changes in the stainless steel samples combining ECT and DC magnetization, therefore the solution can be likewise applied for geometrical defects to identify metal losses of the corrosion process.

REFERENCES

[1] Reber K, Boenisch A. Advanced Electromagnetic Technology and Tools for Subsea Inspection, Subsea Pipelines Integrity Management Conference 2012.

[2] Camerini C, Sacramento R, Areiza M, Rocha A, Santos R, Rebello J, Pereira G. Eddy current techniques for super duplex stainless steel characterization, Journal of Magnetism and Magnetic Materials 2015; 388: 96-100, ISSN 0304-8853. https://doi.org/10.1016/j.jmmm.2015.04.034

[3] Xie S, Duan Z, Li J, Tong Z, Tian M and Chen Z. A novel magnetic force transmission eddy current array probe and its application for nondestructive testing of defects in pipeline structures. Sensors and Actuators A: Physical 2020; 309: 112030. https://doi.org/10.1016/j.sna.2020.112030

[4] Zhao Y, Qi P, Xie Z, Bai P, Chen HE, Xie S, and Chen Z. A new array eddy current testing probe for inspection of small-diameter tubes in Tokamak fusion devices. Fusion Engineering and Design 2020; 157: 111627. https://doi.org/10.1016/j.fusengdes.2020.111627

[5] Zhao Y, Qi P, Xie Z, Bai P, Chen HE, Xie S and Chen Z. A new array eddy current testing probe for inspection of small-diameter tubes in Tokamak fusion devices. Fusion Engineering and Design 2020; 157: 111627. https://doi.org/10.1016/j.fusengdes.2020.111627

[6] James R, Faisal Haider M, Giurgiutiu V, and Lilienthal D. A simulative and experimental approach toward Eddy current nondestructive evaluation of manufacturing flaws and operational damage in CFRP composites. Journal of Nondestructive Evaluation, Diagnostics and Prognostics of Engineering Systems 2020; 3(1). https://doi.org/10.1115/1.4044722

[7] Sophian A, Tian GY, Taylor D and Rudlin J. Electromagnetic and eddy current NDT: a review. Insight 2001; 43(5): 302-306.

[8] Hollaus K and Schöberl J. Some 2-D multiscale finite-element formulations for the eddy current problem in iron laminates. IEEE Transactions on Magnetics 2018; 54(4): 1-16. https://doi.org/10.1109/TMAG.2017.2777395

[9] Oh S, Choi G, Lee D, Choi M and Kim K. Analysis of Eddy-Current Probe Signals in Steam Generator U-Bend Tubes Using the Finite Element Method. Applied Sciences 2021; 11(2): 696. https://doi.org/10.3390/app11020696

[10] Barrarat F, Rayane K, Helifa B and Lefkaier IK. Characterization of subsurface cracks in eddy current testing using machine learning methods. International Journal of Numerical Modelling: Electronic Networks, Devices and Fields 2021; e2876. https://doi.org/10.1002/jnm.2876

[11] Li S and Cui X. An edge-based smoothed finite element method for nonlinear magnetostatic and eddy current analysis. Applied Mathematical Modelling 2018; 62: 287-302. https://doi.org/10.1016/j.apm.2018.06.003

[12] Tian C, Zhong Y, Wei L, Lei Y, Chen B, Gao Y and Yuan J. A coupled method for evaluating eddy current loss of NdFeB permanent magnets in a saturated core fault current limiter. IEEE Transactions on Magnetics 2017; 53(6): 1-4. https://doi.org/10.1109/TMAG.2017.2664828

[13] Foucher F, Kalai A, Kelb W, Ramadan S and Delemontez J. A modeling study of the SLOFECTM Eddy Current system. In 19th World Conference on Non-Destructive Testing 2016.

[14] Deng Z, Sun Y, Kang Y, Song K and Wang R. A permeability-measuring magnetic flux leakage method for inner surface crack in thick-walled steel pipe. Journal of Nondestructive Evaluation 2017; 36(4): 1-14. https://doi.org/10.1007/s10921-017-0447-z

[15] Horai S, Hirata K & Niguchi N. Flux-focusing eddy current sensor with magnetic saturation for detection of water pipe defects. International Journal of Applied Electromagnetics and Mechanics 2016 52(3-4): 1231-1236. https://doi.org/10.3233/JAE-162099

[16] Rifai D, Abdalla AN, Khamsah N, Aizat M and Fadzli M. Subsurface defects evaluation using eddy current testing. Indian J. Sci. Technol 2016; 9: 10-17485. https://doi.org/10.17485/ijst/2016/v9i9/88724

[17] Jackson JD. Classical electrodynamics 1999.

[18] Bönisch A, Dijkstra FH and de Raad JA. Magnetic flux and SLOFEC inspection of thick walled components. In Proc. 15th World Conference on Nondestructive Testing 2000; 15: 1-8.

[19] Ida WLN, Palanisamy R. Eddy Current Probe Design Using Finite Element Analysis, Materials evaluation 1983; 41: 1389-1493.

[20] Mengbao Fan, Pingjie Huang, Bo Ye, Dibo Hou, Guangxin Zhang, Zekui Zhou. Analytical modeling for transient probe response in pulsed eddy current testing, NDT & E International 2009; 42(5): 376-383. https://doi.org/10.1016/j.ndteint.2009.01.005

[21] Villone F. Simulation of thin cracks with finite resistivity in eddy current testing, IEEE Transactions on Magnetics 2000; 36(4): 1706-1709. https://doi.org/10.1109/20.877771

[22] Santandrea L and Le Bihan Y. Using COMSOL-multiphysics in an eddy current non-destructive testing context. In Proceedings of the COMSOL Conference 2010.

Received on 18-03-2021 Accepted on 12-05-2021 Published on 16-07-2021

DOI: https://doi.org/10.31875/2410-4701.2021.08.2